ELSEVIER

Polymer 42 (2001) 9903–9908

polymer

www.elsevier.com/locate/polymer

The moisture vapour transmission rate of block co-poly(ether–ester) based breathable films. 2. Influence of the thickness of the air layer adjacent to the film

Alexander Stroeks*

DSM Research, P.O. Box 18, 6160 MD Geleen, The Netherlands

Received 25 June 2001; accepted 6 August 2001

Abstract

Water permeability is an important item for many applications of block co-poly(ether–ester) films. For segments, such as protective clothing or construction applications, water permeability is not only governed by the polymer film, but also by stagnant air layers surrounding the film. We interpreted this barrier effect by a series of permeability experiments in a standardised ASTM E96B test, varying systematically the air layer thickness adjacent to the block co-poly(ether–ester) film. Furthermore, we developed a mass transport model describing the water transport in the polymer film and air layer. Experimentally, we observe two regimes. For a relatively small air layer thickness, the water permeability varies strongly with varying air layer thickness, for a relatively large thickness there is hardly any dependence. With the model at hand, we rationalise these effects. For the first regime, the water transport in the air layer is diffusion driven, in the second regime it is of a convective nature. The strong water permeability dependency is interpreted in terms of the water sorption isotherm of the polymer material. The predictive description of the model is of a quantitative nature. © 2001 Elsevier Science Ltd. All rights reserved.

Keywords: Water permeability; Block co-poly(ether–ester) films; Mass transport model

1. Introduction

DSM is producer of a class of thermoplastic elastomer materials (TPEs) commercialised under the trade name Arnitel®. These materials are based on segmented block co-poly(ether–ester) systems, with the ester polybutyleneterephthalate forming the hard blocks while the soft blocks are propyleneoxide or butyleneoxide based. An important area of application for these materials is breathable film, i.e. a film that possesses a rather high permeability towards water vapour while acting as a barrier towards liquid water. Examples of applications for breathable films are: clothing, protective apparel, diapers, feminine hygiene and roofing membranes.

There is a large variety of test methods which can be used for measuring the water permeability or moisture vapour transmission rate (MVTR) of breathable films. Usually, different market segments require different test methods. For some applications, there is direct contact with the film and liquid water, for some applications the film is in contact with an atmosphere with a certain relative humidity. In order to mimic these real life situations, several rather pragmatic standardised test methods have been developed. These tests differ strongly in conditions like: humidity on both sides of the film, temperature, direct contact of water with the film or not, etc. In the first paper of this series [1], we presented a model to predict MVTR values for two types of frequently used tests; the so-called inverted cup test (ASTM E96BW) and upright cup test (ASTM E96B test), see Fig. 1. In both cases, the cups are placed in an equilibrated chamber at 38°C and a relative humidity of 50%. The inverted cup test mimics real life conditions for which there is direct contact between liquid water and the film. The upright cup test simulates conditions where the film is in contact with two atmospheres with a different relative humidity. For a given film, the MVTR value for the upright cup test is smaller or equal to the MVTR measured according to the inverted cup test. This effect is attributed [1] to the fact that the extra air layer forms an additional barrier towards water transport reducing the overall water flux. With the model at hand, we can predict this effect quantitatively. In Ref. [1], however, we focused exclusively on an air layer thickness of 7.5 cm and concluded for the given cases that transport in this layer was driven by free convection. For real life applications,

---

* Tel.: +31-46-4761840; fax: +31-46-4767569.
E-mail address: alexander.stroeks@dsm.com (A. Stroeks).

PII: S0032-3861(01)00565-1

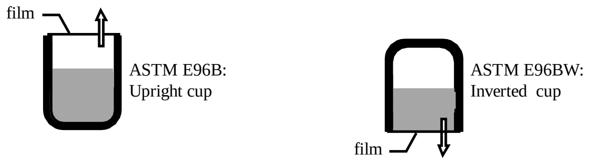

Fig. 1. Schematic representation of E96B and E96BW MVTR tests.

however, this air layer thickness is not fixed and will vary from one application to another. We performed an extended study in which we simulated this real life situation. We performed a series of experiments varying the air layer thickness in the upright cup test. Furthermore, we investigated whether our model was capable of predicting the effect of this variation on the overall MVTR.

2. Experimental

2.1. Experimental set-up and grade information

One type of Arnitel grade was used in this study, known as Arnitel PM380. For this grade, the ether is an oligomeric linear propyleneoxide. The hard segments consist of oligomeric butyleneterephthalate. Cast film was produced on a Battenfeld 45 mm extruder, equipped with a Verbruggen 250 mm slit die with a die opening of 300 μm. The film was cast on a chill roll which was set at a temperature of 12°C. The film thickness was varied by changing the speed of the chill roll and wind-up unit.

PM380 type Arnitel films with thicknesses in the range 28–34 μm were placed between cup and ring, see Fig. 2. The whole set-up was placed upright in a conditioned chamber at 38°C and a relative humidity of 50%. The atmosphere around the cup is ventilated, so there is no mass transport barrier outside the cup. The air layer thickness in the cup at the start of each experiment is changed by a variation of the amount of liquid water.

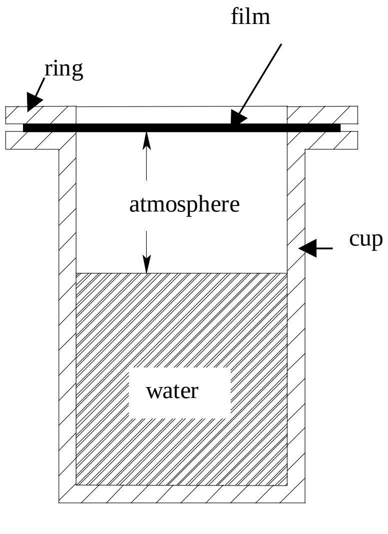

Fig. 2. Schematic representation of the cup in an upright cup test (ASTM E96B test).

Table 1
Practical information for the experimental series

Exp. number	Film thickness (μm)	Average air layer thickness (mm)	MVTR (g/m^2 s)
1	27.8	84	0.01684
2	28.8	75	0.01556
3	34.2	65	0.01634
4	32.2	56	0.01691
5	28.8	51	0.01648
6	31.6	48	0.01698
7	32.2	42	0.01726
8	31.6	37	0.01754
9	31.8	32	0.01875
10	35.8	28	0.01798
11	32.4	26	0.01691
12	34.6	24	0.01684
13	31.0	21	0.01790
14	29.6	19	0.01988
15	31.2	17	0.01896
16	35.4	15	0.02002
17	32.6	12	0.02094
18	35.0	10	0.02306
19	34.4	8	0.02412
20	34.4	4	0.02815

An experiment takes typically 25 h, the weight reduction is determined for intermediate times. After the experiment, the air layer thickness is determined again. The difference between the air layer thickness at the start and at the end of each experiment is typically 2 mm. The average value of the air layer thickness for each experiment, together with the Arnitel film thickness, is given in Table 1.

2.2. Experimental results

The amount of permeated water versus time for the experimental series is determined gravimetrically. The MVTR values, as determined under steady state conditions, are given in Table 1 and are plotted against air layer thickness in Fig. 3. The general trend is a reduction of the MVTR value with increasing air layer thickness. The reason is that

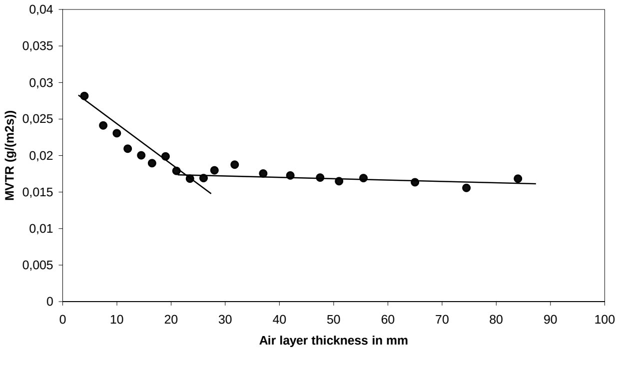

Fig. 3. Experimental MVTR values versus air layer thickness (indicated lines are guides for the eye).

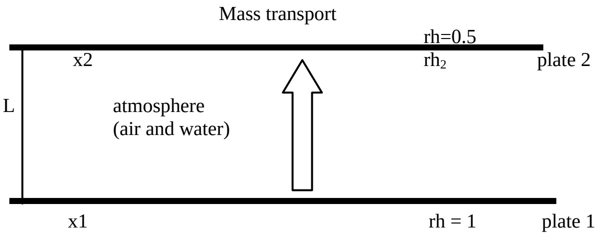

Fig. 4. Schematic representation of the atmosphere layer between two horizontal parallel plates.

besides the polymer film also the stagnant air layer forms a barrier towards mass transport of water. An increase of the air layer thickness leads to an increase in mass transport resistance and consequently in a reduction of the MVTR value. The interesting observation is that apparently two regimes can be distinguished. For air layer thicknesses between 0 and 30 mm, the MVTR drops rather rapid with increasing thickness. For an air layer thickness of 30 mm and more, the descent is more gradual. In the next paragraph, this behaviour will be interpreted in terms of a mass transport model.

3. Description of the mass transport model

The model to describe the water transport in the PM380 polymer film and in the adjacent stagnant air layer has been described in detail before [1]. Therefore, the model will be described here rather briefly. In fact, we have a situation where we have two barriers towards mass transport that are connected in series. The first barrier forms the polymer film, the second barrier the air layer, see Fig. 2. The difference in relative humidity forms the driving force for the water to migrate from the water surface to the atmosphere of the conditioned chamber. At the liquid water surface, this relative humidity is 100% and in the atmosphere outside the cup, it is 50%. The transport of water in the film is described in terms of simple Fickian diffusion behaviour with an overall diffusion coefficient independent of the location in the film or alternatively the water concentration. So,

$$\mathrm{MVTR} = D_{\mathrm{film}} \frac{c_2 - c_1}{l} \tag{1}$$

with

D_{film}: the diffusion coefficient for water in a PM380 matrix
c_1: the concentration of water solved in the polymer film at the upper film surface which is in equilibrium with the atmosphere with a relative humidity of 50%
c_2: the concentration of water solved in the polymer film at the lower film surface which is in equilibrium with the atmosphere with a relative humidity which is a priori not known
l: the film thickness

The value of the diffusion coefficient for water in PM380 is 2.3644×10^{-11} m^2/s, see Ref. [1].

The relation between the solved amount of water in the film and the relative humidity in the atmosphere is described by the sorption isotherm. In Ref. [1], we applied a thermodynamic model developed by Brown [2] to describe the sorption isotherm for water in PM380. In fact, this model of Brown is a combination of a Zimm–Lundberg [3,4] cluster type approach and the classical Flory–Huggins [5] model, and in the case of PM380 leads, under given circumstances, to the following equilibrium relation between weight fraction of water in the polymer material, c, and relative humidity in the atmosphere, rh:

$$\frac{1}{c} = \frac{136.31}{\mathrm{rh}} - 118.77 \tag{2}$$

Combining Eqs. (1) and (2), and recognising that at the top of the film the relative humidity of the atmosphere equals 0.5 and at the bottom the relative humidity rh$_2$ is not known, we obtain:

$$\mathrm{MVTR}_{\mathrm{film}} = \frac{D_{\mathrm{film}}}{l}\left[\left(\frac{1}{\frac{136.31}{\mathrm{rh}_2} - 118.77}\right) - 0.0065\right] \tag{3}$$

The value for rh$_2$ depends on the ratio of the mass transport barrier of the air layer and the mass transport resistance of the polymer film. In case this ratio equals zero, rh$_2$ equals 1 and with Eq. (3), we are able to predict the MVTR. For finite air layer thicknesses, however, the ratio is larger than zero and rh$_2$ is a priori not known. We also have to describe the mass transport of water in the air layer.

In order to do so, we revert to a classical approach, known as the Bénard problem [6,7]. This problem deals with the analysis of the stability of heat transport of a liquid or a gas between two horizontal plates, schematically sketched in Fig. 4. We make use of the analogy between transport of mass and heat [8] and furthermore, we reduce the cup geometry to the situation of two horizontal plates. Consider a cavity containing an atmosphere, consisting of air and water vapour. Plate 1 represents the liquid water surface, which is in direct contact with an atmosphere with a relative humidity of 1. Plate 2 is the polymer film, which is in downward contact with an atmosphere with a lower relative humidity. Upward the relative humidity of the atmosphere is 0.5. There is an upward driving force for water transport due to a difference in water activity (water activity or alternatively relative humidity in upward position decreases). Transport of water may take place via a diffusion process in a stable situation or by free convection induced by instabilities in the system. The essential drive for instabilities to occur is the density difference of the gas in vertical position and gravity. Under isobaric conditions, the density of the atmosphere at plate 1 is lower compared to the atmosphere at plate 2 because of the higher relative humidity at plate 1. Stabilising factors are the diffusion process, which tends to dampen perturbations, and the viscosity of the gas. For small differences in relative humidity, the stabilising factors are dominant over the destabilising ones resulting in a diffusional transport mechanism for water in the atmosphere. For somewhat larger differences in relative humidity, destabilising factors start to take over resulting in free convection manifesting itself by the occurrence of stable vortices that are laminar in nature. For even larger differences, free convection will become turbulent manifested by irregular and unstable vortices. The discussed stabilising and destabilising factors can be expressed in a single dimensionless number, the so-called Rayleigh number which is defined as the product of the Grashof and Schmidt number [8]:

$$\begin{aligned}\mathrm{Ra} &= \mathrm{Gr}_{\mathrm{ab}}\mathrm{Sc} \\ &= \frac{\rho^2 \xi g L^3 (x_1 - x_2)}{\mu^2}\frac{\mu}{\rho D} \quad \text{with } \xi = \frac{-1}{\rho}\left(\frac{\partial \rho}{\partial x}\right)_{p,T} \\ &= \frac{-\left(\frac{\partial \rho}{\partial x}\right)_{p,T} g L^3 (x_1 - x_2)}{\mu D} \qquad (4)\end{aligned}$$

Symbols and their numerical values under the given circumstances (38°C, 1 bar) are defined in Table 2.

With these numerical values, the expression for the Rayleigh number becomes:

$$\mathrm{Ra} = 5.44516 \times 10^8 (1 - \mathrm{rh}_2) L^3 \qquad (5)$$

The critical Rayleigh number, marking the transition from diffusional transport to transport by free convection, is given by [7]:

$$\mathrm{Ra}_{\mathrm{c}} \cong 1700 \qquad (6)$$

Table 2
Explanatory table

Abbreviation	Explanation	Numerical value under given circumstances
$\mathrm{Gr}_{\mathrm{ab}}$	Grashof number for mass transfer	–
Sc	Schmidt number	–
ρ, dry	Density dry atmosphere	1.1347×10^3 g/m^3 [9]
ρ, rh = 1	Density atmosphere rh = 1	1.1065×10^3 g/m^3
G	Gravitational acceleration	9.81 m/s^2
L	Air layer thickness	Varying
μ	Viscosity atmosphere	1.891×10^{-2} g/ms [9]
D	Diffusion coefficient of atmosphere	2.683×10^{-5} m^2/s [9]
c_1	Concentration water in atmosphere at plate 1 (rh = 1)	46.24 g/m^3 [10]
c_2	Concentration water in atmosphere at plate 2	A priori unknown
x_1	Mole fraction water in atmosphere at plate 1 (rh = 1)	0.006565
x_2	Mole fraction water in atmosphere at plate 2	A priori unknown

For Rayleigh numbers above this critical value, instability factors start to dominate and free convection dominates the mass transport process. The Rayleigh number, marking the transition from free convection with a laminar character to a turbulent nature, for our specific case is given by [10]:

$$\mathrm{Ra}_{\mathrm{t}} = 2 \times 10^7 \qquad (7)$$

Following the dimensionless analysis of free convection [7], the Nusselt number for mass transport can be expressed as a function of the Rayleigh number:

$$\mathrm{Nu}_{\mathrm{ab}} = \mathrm{Nu}_{\mathrm{ab}}(\mathrm{Ra}) = \frac{kL}{D} \qquad (8)$$

with k the mass transfer coefficient.

For our specific case, the following empirical relations can be applied [7]:

$$\text{diffusional transport}: \quad \mathrm{Nu}_{\mathrm{AB}} = 0.54\mathrm{Ra}_{\mathrm{c}}^{1/4} \approx 3.47 \qquad (9)$$

$$\text{free convection, laminar} \quad \mathrm{Nu}_{\mathrm{AB}} = 0.54\mathrm{Ra}^{1/4} \qquad (10)$$

$$\text{free convection, turbulent} \quad \mathrm{Nu}_{\mathrm{AB}} = 0.14\mathrm{Ra}^{1/3} \qquad (11)$$

Now we are in a position to estimate the Nusselt number, it is possible to express the transport phenomena in the air layer in terms of a mass transfer coefficient. The flux in the air layer is described by

$$\mathrm{MVTR}_{\mathrm{atm.}} = k\Delta c \qquad (12)$$

with Δc the concentration difference of water in the atmosphere at plates 1 and 2.

So, in the case mass transport in the air layer is dominated by diffusional transport, we obtain:

$$\mathrm{MVTR}_{\mathrm{atm.}} = 3.47\frac{D}{L}46.24(1 - \mathrm{rh}_2) \qquad (13)$$

For laminar free convection, the flux is described by:

$$\mathrm{MVTR}_{\mathrm{atm.}} = 0.54\frac{D}{L}\mathrm{Ra}^{1/4}46.24(1 - \mathrm{rh}_2) \qquad (14)$$

and for turbulent free convection:

$$\mathrm{MVTR}_{\mathrm{atm.}} = 0.14\frac{D}{L}\mathrm{Ra}^{1/3}46.24(1 - \mathrm{rh}_2) \qquad (15)$$

Under stationary conditions:

$$\mathrm{MVTR}_{\mathrm{atm.}} = \mathrm{MVTR}_{\mathrm{film}} \qquad (16)$$

So, combining expressions (3), (5), (13)–(16), the ultimate expressions for the MVTR become, in the case of diffusional transport in the atmosphere:

$$\frac{D_{\mathrm{film}}}{l}\left[\left(\frac{1}{\frac{136.31}{\mathrm{rh}_2} - 118.77}\right) - 0.0065\right] = 3.47\frac{D}{L}46.24(1 - \mathrm{rh}_2) \qquad (17)$$

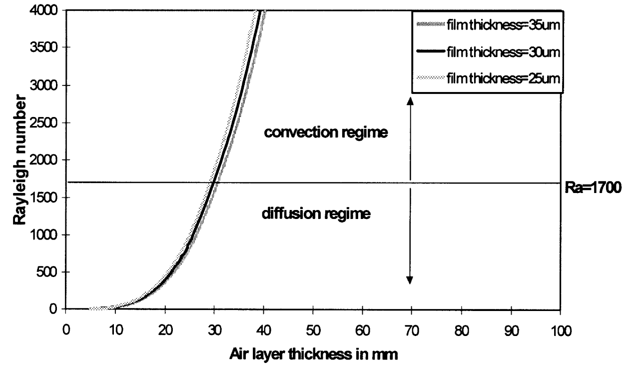

Fig. 5. Computed Rayleigh number versus air layer thickness for three indicated Arnitel PM380 film thicknesses in an E96B test.

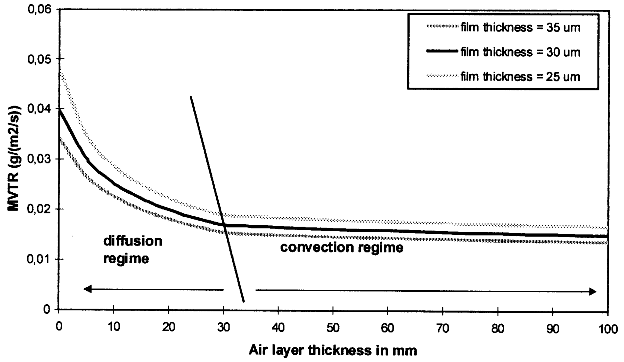

Fig. 6. Predicted MVTR versus air layer thickness for three indicated Arnitel PM380 film thicknesses in an E96B test.

For laminar free convection:

$$\frac{D_{\text{film}}}{l}\left[\left(\frac{1}{\dfrac{136.31}{\text{rh}_2}-118.77}\right)-0.0065\right]$$

$$=0.54\frac{D}{L}\left(5.44516\times 10^{8}\frac{1-\text{rh}_2}{L^3}\right)^{1/4}46.24(1-\text{rh}_2) \quad (18)$$

For turbulent driven mass transport:

$$\frac{D_{\text{film}}}{l}\left[\left(\frac{1}{\dfrac{136.31}{\text{rh}_2}-118.77}\right)-0.0065\right]$$

$$=0.14\frac{D}{L}\left(5.44516\times 10^{8}\frac{1-\text{rh}_2}{L^3}\right)^{1/3}46.24(1-\text{rh}_2) \quad (19)$$

We take the following strategy. For a certain experimental thickness of the air layer, these three equations are solved with respect to rh_2, the only unknown parameter. The value of the Rayleigh number, computed according to Eq. (5), tells us what is the prevailing mechanism for mass transport of water in the air layer. On the basis of this information, only one of three equations (Eqs. (17)–(19)) remains applicable to the problem at hand. The remaining equation gives us the MVTR value for the specific test with the given air layer thickness.

It should be clear that no adjustable parameter is used to predict the following quantities:

- the prevailing transport mechanism in the air layer
- the value of the relative humidity in the atmosphere at the lower side of the polymer film
- the overall value of the MVTR

4. Model predictions and comparison with experimental results

In the first instance, we solve Eqs. (17)–(19) for an air layer thickness between 0 and 100 mm and for three values of the Arnitel PM380 film thickness (25, 30 and 35 μm) which match the experimental film thickness regime. On the basis of the value of the Rayleigh parameter (Eqs. (5)–(7)), we are in a position to decide what transport mechanism governs mass transport in the air layer and decide whether Eq. (17), (18) or (19) is appropriate to compute rh_2 and MVTR.

In Fig. 5, the computed Rayleigh number is presented versus the air layer thickness. The observation is that for an air layer thickness of approximately 30 mm, the Rayleigh number passes $\text{Ra}_\text{c} = 1700$. In the studied regime, the number does not exceed Ra_t. This means that for air layer thicknesses below 30 mm, the mass transport mechanism in the air layer is governed by diffusion, beyond 30 mm the mass transport process is determined by free convection that is laminar in nature. A turbulent regime is not reached. For thin films, the convection driven regime is achieved for smaller air layer thicknesses, although for the studied regime this effect is rather small.

In Fig. 6, the computed MVTR is plotted versus the air layer thickness. The observation is that in the diffusion regime (air layer thickness <30 mm) the MVTR falls off rather steep. Increasing the air layer thickness from 0 until 30 mm leads to a reduction of the MVTR with roughly a factor 2. Beyond a thickness of 30 mm, the convection dominated regime is entered and the dependency between MVTR and air layer thickness is much less pronounced. In this regime, an increase in air layer thickness hardly leads to a further reduction of the water flux.

The predicted relative humidity of the atmosphere direct in contact with the lower film side (rh_2) is given in Fig. 7. Here, a steep descent is observed from a relative humidity of 100% to a value in the regime 87–89% upon an increase of the air layer thickness from 0 to 30 mm. Apparently, this has a large effect on the overall MVTR, a drop of a factor 2 is observed as described before. Reason for this large drop of the MVTR is the form of the sorption isotherm for PM380 as plotted in Fig. 8 according to Eq. (2). On the upper side of the film, we apply a relative humidity of 50%. On the lower side, it is varied between 100 and 87%. In this latter regime, the amount of water solved in the PM380 Arnitel material

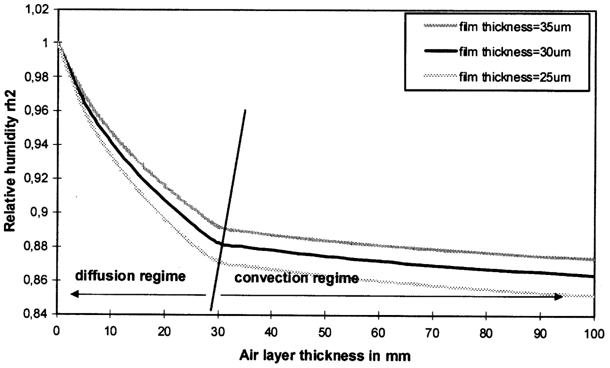

Fig. 7. Predicted relative humidity of the atmosphere direct in contact with the lower film side (rh_2) versus air layer thickness for three indicated Arnitel PM380 film thicknesses in an E96B test.

varies very strongly, which is the reason for the vast change of MVTR upon changing the air layer thickness between 0 and 30 mm.

In Fig. 9, the experimental MVTR series is directly compared with the predicted one. In the predicted series, the exact thickness of each individual film was taken into account. Furthermore, the predicted trend for three standard film thicknesses is displayed. The experimental and predicted points are somewhat scattered, because the experimental film thickness was not constant for all films but varied in the range of 28–34 μm. As stated before, the diffusion and the convection regime are clearly reflected by the experimental points. The observed transition is close to an air layer thickness of 30 mm as predicted by the mass transport model. The experimental points, with each point characterised by a specific film thickness, are described in a quantitative manner by the model. This is very gratifying.

5. Conclusions

- We performed a series of water permeability experiments in a standardised ASTM E96B test varying systematically the thickness of the air layer adjacent to the block co-poly(ether–ester) film. By this, we mimic applications for which the water permeability is not only governed by the polymer film but also by surrounding stagnant air layers. Furthermore, we developed a mass transport model describing water transport in the polymer film and air layer.

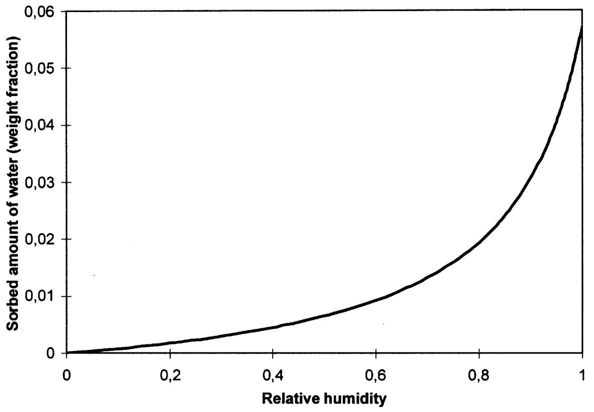

Fig. 8. Sorption isotherm for water in Arnitel PM380.

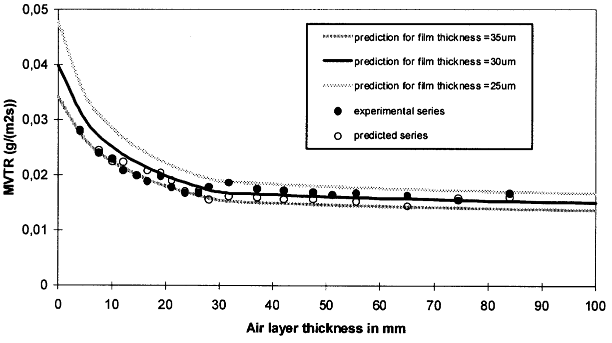

Fig. 9. Experimental and predicted MVTR versus air layer thickness in an E96B test.

- Experimentally, we observe two regimes. For relatively small air layer thicknesses, the water permeability varies strongly with varying air layer thickness, for relatively large thickenesses there is hardly any dependence.
- With the model at hand we rationalise these effects. For the first regime, the water transport in the air layer is diffusion driven, in the second regime it is of a convective nature. The strong water permeability dependency is interpreted in terms of the water sorption isotherm of the polymer material. The predictive description of the model is of a quantitative nature.

Acknowledgements

R. Vos is acknowledged for performing the permeability measurements.

References

[1] Stroeks A, Dijkstra K. Polymer 2001;42:117.

[2] Brown G. In: Rowland SP, editor. Water in polymers, ACS symposium series, vol. 127. Washington, DC: American Chemical Society, 1980.

[3] Zimm BH, Lundberg JL. J Phys Chem 1956;60:425.

[4] Zimm BH. J Chem Phys 1953;21:934.

[5] Flory PJ. Principles of polymer chemistry. Ithaca, NY: Cornell University Press, 1953.

[6] Bénard H. Rev Gén Sci Pure Appliq 1900;11:1261.

[7] Agassant J-F, Avenas P, Sergant J-Ph, Carreau PJ. Polymer processing, principles and modeling. Munich: Hanser, 1991. p. 369.

[8] Bird RB, Stewart WE, Lightfoot EN. Transport phenomena. New York: Wiley, 1960.

[9] Landolt-Börnstein. In: Hellwege KH, editor. Zahlenwerte und functionen am Naturwissenschaften und Techniek. Berlin: Springer, 1975.

[10] Schmidt E. In: Grigull H, editor. Properties of water and steam in SI-units. Berlin: Springer, 1989.